

Modeling and Elimination of Atenolol on Granular Activated Carbon in Fixed Bed Column

Sotelo, J.L. *, Rodríguez, A., Álvarez, S. and García, J.

Grupo de Catálisis y Procesos de Separación (CyPS), Departamento de Ingeniería Química,
Facultad de Ciencias Químicas, Universidad Complutense de Madrid, Avda. Complutense
s/n, 28040 Madrid, Spain

Received 29 Oct. 2011;

Revised 19 May 2012;

Accepted 26 May 2012

ABSTRACT: The emerging contaminants are commonly derived from municipal, agricultural, and industrial wastewater sources and pathways. These compounds are polar and poorly biodegradable. The dynamic removal of atenolol from aqueous solutions by activated carbon in fixed bed column systems was investigated. As far as we know, this is the first study reporting the decontamination by adsorption in fixed bed of solutions containing atenolol, as model compound of β -blockers, which are pharmaceutical pollutants with a high occurrence in natural waters. The performance of fixed bed columns was described through the breakthrough curves obtained from column experiments. The Bohart-Adams, Thomas and Yoon-Nelson models were applied to predict different parameters of the column like service time (Bohart-Adams model), adsorption capacity (Thomas model) and time required for 50% breakthrough (Yoon-Nelson model). Also, the theoretical breakthrough adsorption curve has been obtained. For the last, an industrial scale adsorber was designed from characteristic parameters of the breakthrough curves obtained from experimental data.

Key words: Adsorption, Activated carbon, Atenolol, Fixed bed, Water

INTRODUCTION

The human drugs are introduced primarily after medication via urinal or fecal excretion into sewage treatment plants, where they are eliminated to great extent (Postigo *et al.*, 2010; Bolong *et al.*, 2009; Ternes *et al.*, 2002; Akbarpour Toloti and Mehrdadi, 2011). However, those pharmaceuticals which are polar and poorly biodegradable are finally emitted into surface waters, because conventional wastewater treatment plants containing activated sludge process showed incomplete removal of the most micropollutants. The research on the presence of these compounds in the environment has been active particularly in Europe and USA (Carballa *et al.*, 2008; Lishman *et al.*, 2006; Vergili *et al.*, 2009). Beta-blockers, such as atenolol, acebutolol, oxprenolol, and others, are used extensively as non-prescription drugs (Arvand *et al.*, 2008), and residues of these compounds have been detected in the aquatic environment (Gros *et al.*, 2006). Some of these β -blockers may be eliminated by ozonation (Hua *et al.*, 2006; Beltrán *et al.*, 2009) since their amine function constitutes site of attack for O_3 . Other reports use advanced oxidation processes for the treatment of pharmaceutical waste (Benítez *et al.*, 2011). Measured by volume of use per capita, Americans consume more prescription drugs than any other country, Spain is the

second country in the world in drug consumption (www.msps.es) and significant concentrations of these pharmaceuticals have been detected in municipal sewage. Fixed bed adsorption is widely used for purifying liquid mixtures, especially industrial waste effluents and it is simple to operate and can be scaled-up from a laboratory process. In a little over two decades, granular activated carbon (GAC) was extensively used for waste and water treatment (Sotelo *et al.*, 2004; Westerhoff *et al.*, 2005). In this work we have studied the removal of atenolol in water by adsorption. To our knowledge, this is the first study on atenolol adsorption in fixed bed with granular activated carbon. Therefore, in order to predict the column breakthrough or the shape of the adsorption wave front, it is essential to study the operation on a fixed bed column (Goel *et al.*, 2005). Various methods for the design of fixed-bed columns have been suggested, such as the bed depth service time approach (BDST) in the Bohart-Adams model, the Thomas and the Yoon-Nelson models have been tried elsewhere (McKay, 1996; Kundu and Gupta, 2007). Also, the analysis of experimental breakthrough curves obtained allows to obtain parameters to be considered in the design of an industrial-scale adsorber to be located in a wastewater treatment plant.

*Corresponding author E-mail: jose.sotelo@quim.ucm.es

MATERIALS & METHODS

Atenolol was purchased from Sigma-Aldrich (Steinheim, Germany), in analytical purity and used as received in the experiments. Solutions of atenolol of appropriate concentration were prepared by diluting a stock solution. The main characteristics are shown in Table 1. Granular activated carbon, Calgon Filtrasorb 400, having a specific area of 997.0 m²/g, external area of 384 m²/g, microporous volume of 0.26 cm³/g and pH_{PZC} = 7.6 has been used as adsorbent ($\rho_p = 453.6$ g/L, $\varepsilon_p = 0.410$). Before use, the adsorbent was washed with water to remove surface impurities, followed by drying at 100 °C for 48 hours. The fraction between 0.5 to 0.589 mm (average particle size) was selected by sieving. To obtain adsorption equilibrium isotherm data corresponding to the granular activated carbon, aqueous phase adsorption experiments were performed in 250 mL glass vials. The suspensions containing different doses of adsorbent and the solutions of atenolol were shaken with a magnetic stirrer. In all experiments, the vials were agitated on a fixed speed rotator at room temperature (25±1 °C).

Fixed bed column experiments were conducted using borosilicate glass columns of 6 mm i.d. and 30 cm length. The column was packed with the granular activated carbon and then, the column was filled with a layer of glass balls (1 mm in diameter) to compact the mass of adsorbent and to avoid dead volumes. The influent solution to the column was pumped using a Dinko multichannel peristaltic pump, model D25V. The column studies were conducted to evaluate the effect of different bed weights on breakthrough curves. Fixed bed experiments were carried out under the operational conditions shown in Table 2. The influent solutions were passed in the down-flow mode through the bed. The effluent was collected at time intervals and its concentration was determined by HPLC, using a Varian Chromatograph equipped with a 335 UV-Vis Photodiode Array Detector (PAD) and a Mediterranean C18 column (5µm, 250 mm x 4.6 mm i.d.). An isocratic

elution of acetonitrile (A) and aqueous solution (B) was used (30% A, 70% B v/v), with a mobile phase flow rate of 1.0 mL/min, and an injection volume of 100 µL.

RESULTS & DISCUSSION

In order to obtain the adsorption isotherm, additional batch experiments were carried out to find out the equilibrium data. In this sense, experiments were conducted for various time intervals to determine the time required to reach adsorption equilibrium (Fig. 1). The equilibrium state was considered reached after about 23 hours, since the variations in equilibrium adsorption capacity did not change more than 5%. This contaminant, as seen in Fig. 2, presents an isotherm shape that can be fitted to BET model (Brunauer-Emmett-Teller). This is a theoretical model that assumes that the monolayer is first formed, and then the successive multilayer act as adsorption sites in the process. These isotherms are generally L3-type according to the Giles classification (Giles and Nakhwa, 1962).

Breakthrough curves for atenolol adsorption are shown in Fig. 3. All the breakthrough curves followed a bilayer profile, characteristic of this pollutant in fixed bed operation. It can be observed that breakthrough time increased with increasing the bed height. The breakthrough times, corresponding to $C/C_0 = 0.02$ were found to be 23.8, 78.5 and 82.8 h for the columns operating with bed heights of 8.0, 10.0 and 12.0 cm; respectively. The saturation times (corresponding to $C/C_0 = 0.90$) were found to be 139.8, 221.2 and 280.2 h, respectively. It can be observed that when the bed height increases from 8.0 to 12.0 cm, atenolol had more time to contact with the granular activated carbon that resulted in higher removal efficiency in column (Table 3); so the higher bed column results in a decrease of the solute concentration in the effluent at the same time. The slope of breakthrough curve decreased with increasing bed height (slope at 8 cm = 0.01194 > at 10 cm = 0.00807 > at 12 cm = 0.0077), which resulted in values of the mass transfer zone slightly different each other.

Table 1. Main characteristics of atenolol

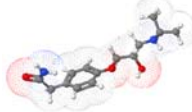
Chemical	CAS #	Formula	M (g/mol)	Therapeutic use
Atenolol (<i>RS</i>)-2-{4-[2-hydroxy-3-(propan-2-ylamino)propoxy]phenyl} acetamide	29122-68-7	 C ₁₄ H ₂₂ N ₂ O ₃	266.336	Hypertension, Angina

Table 2. Operation conditions in fixed bed column experiments

Initial concentration (mg/L)	Bed depth (cm)	Bed weight (g)	Volumetric flow rate (mL/min)
10	8.0	0.8	2.0
10	10.0	1.0	2.0
10	12.0	1.2	2.0

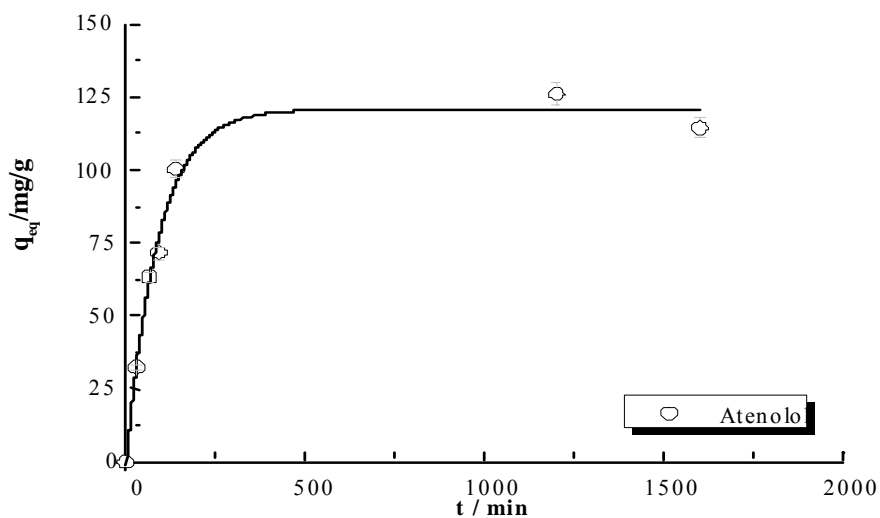


Fig. 1. Equilibrium time for atenolol

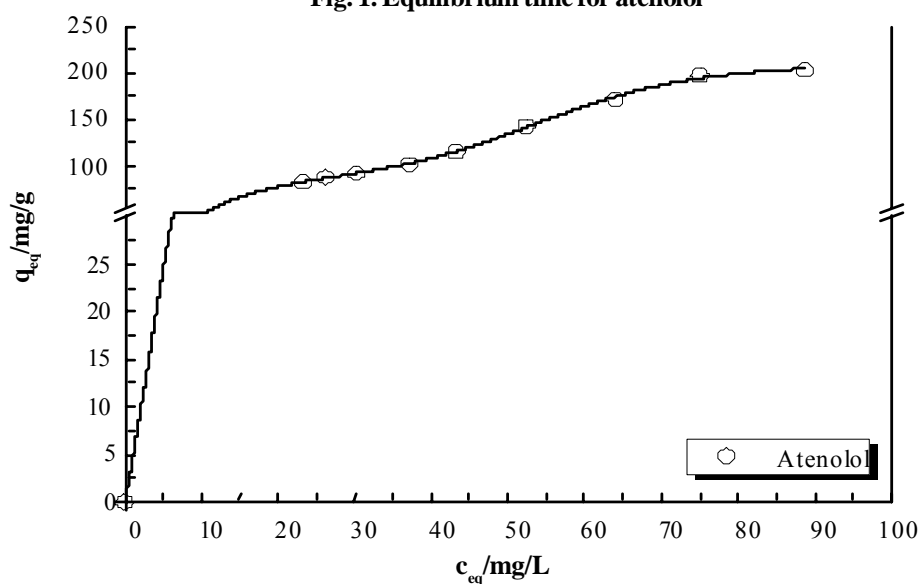


Fig. 2. Adsorption isotherm for atenolol

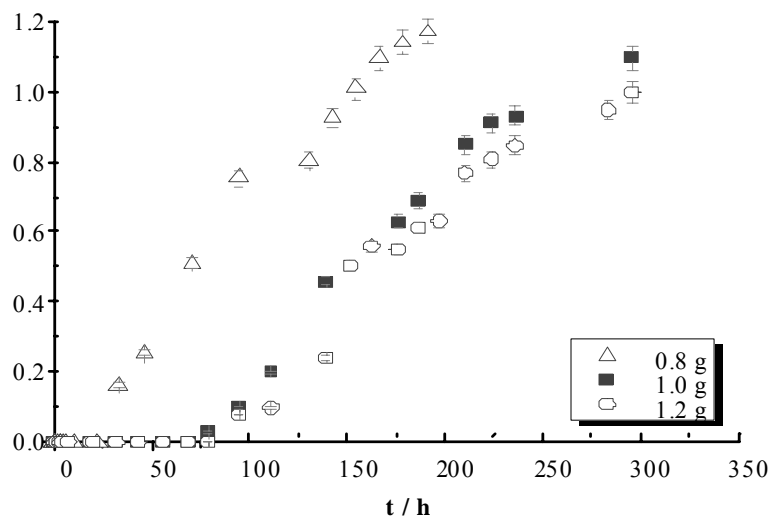


Fig. 3. Breakthrough curves of atenolol removal by granular activated carbon packed columns of different bed weights (initial atenolol conc. = 10 mg.L⁻¹, flow rate = 2.0 mL.min⁻¹)

As it was observed, in general, in the atenolol adsorption studies, the operational conditions influence the mass transfer process and change the mass transfer zone and breakthrough curves. Different parameters, such as adsorption capacities at breakthrough time (q_t) and saturation time (q_s), length of the mass transfer zone (L_{MTZ}), fractional bed utilization (FBU) and removal percentage have been calculated and are shown in Table 3. As seen in Table 3, an increase in bed depth leads to a slight variation in the value of the mass transfer zone, L_{MTZ} . This happens because the lengths tested are not high enough and different from each other to see the profile of a fully developed bed, where to same conditions of flow rate and initial concentration, the value of L_{MTZ} remains constant. From Table 3, it can be observed that in three cases give good removal percentages of atenolol, although slightly better in higher bed height case.

Bohart-Adams model (Bohart and Adams, 1920) established the fundamental equations describing the relationship between C_t/C_0 and t in a continuous system. The Bohart-Adams model is used for the description of the initial part of the breakthrough curve. The expression is the following:

$$\ln\left(\frac{C_0}{C_B} - 1\right) = \ln e^{K \cdot N_0 \cdot \frac{x}{V}} - K \cdot C_0 \cdot t \quad (1)$$

where, C_0 is the initial concentration of solute (mg.L^{-1}); C_B is the desired concentration of solute at breakthrough time (mg.L^{-1}); K is the adsorption rate constant ($\text{L.mg}^{-1}.\text{h}^{-1}$); N_0 is the adsorption capacity (L.mg^{-1}); x is the bed depth of the column (cm); V is the linear flow velocity of feed to bed (cm.h^{-1}); t is the service time of column under above conditions (h).

The linearized form of the equation is the next expression:

$$t = \frac{N_0}{C_0 \cdot V} x - \frac{1}{C_0 \cdot K} \ln\left(\frac{C_0}{C_B} - 1\right) \quad (2)$$

This equation can be used to determine the service time, t , of a column of bed depth, x , given the values of N_0 , C_0 and K which must be determined for laboratory columns operated over a range of velocity values, V .

The bed service time (BDST) model (Hutchins, 1973) proposed a simple approach to the Bohart-Adams equation as

$$t = a \cdot x + b \quad (3)$$

where,

$$a = \text{slope} = \frac{N_0}{C_0 \cdot V} \quad (4)$$

$$b = \text{intercept} = \frac{1}{C_0 \cdot K} \ln\left(\frac{C_0}{C_B} - 1\right) \quad (5)$$

As it is already mentioned, the breakthrough times (corresponding to $C/C_0 = 0.02$) were found to be 23.8, 78.5 and 82.8 h for 8, 10 and 12 cm bed depth, respectively, and the saturation times (corresponding to $C/C_0 = 0.90$) were found to be 139.8, 221.2 and 280.2 h, respectively. Fig. 4 showed the bed depth vs. service time plot for 2% and 90% saturation of column. The equations of these lines were as follows:

For 90% saturation:

$$t = 35.1 \cdot x - 137.3 \quad (6)$$

For 2% saturation:

$$t = 14.8 \cdot x - 85.8 \quad (7)$$

From the slope and the intercept of the 2% saturation line, design parameters like K and N_0 could be found using Eqs. (4) and (5). The values of K and N_0 were found to be $4.5 \cdot 10^{-3} \text{ L/mg.h}$ and $138.5 \text{ mg atenolol/g GAC}$, respectively, this one similar to the value shown in Table 3. The Thomas model (Thomas, 1944) employs a Langmuir's law isotherm, assumes that film diffusion resistance predominates, and neglects axial dispersion. The linearized form of Thomas model can be expressed as follows:

$$\ln\left(\frac{C_0}{C_t} - 1\right) = \frac{K_T \cdot q_0 \cdot w}{Q} - K_T \cdot C_0 \cdot t \quad (8)$$

where K_T ($\text{L.h}^{-1}.\text{mg}^{-1}$) is the Thomas rate constant; q_0 (mg.g^{-1}) is the equilibrium atenolol capacity per g of the adsorbent; C_0 (mg.L^{-1}) is the inlet atenolol concentration; C_t (mg.L^{-1}) is the outlet concentration at time t ; w (g) is the mass of the adsorbent; Q (mL.min^{-1})

Table 3. Adsorption capacities (q_r , q_s), MTZ, FBU, K_L , a , and removal percentage of atenolol

Parameter	Bed depth (cm) (*)		
	8.0	10.0	12.0
q_r (mg atenolol/ gGAC)	44.8	87.9	103.1
q_s (mg atenolol/ gGAC)	98.5	166.1	158.5
L_{MTZ} (cm)	4.36	4.71	4.19
FBU	0.46	0.53	0.65
Removal percentage, %	83.8	97.2	90.2

(*) Bed depths are equivalent to these bed weights, respectively: 8.0, 10.0 and 12.0 g.

¹⁾ is the flow rate and t is the operation time. The value of C_t/C_0 is the ratio of outlet and inlet atenolol concentrations. Thomas model was applied to the data at C_t/C_0 ratios higher than 0.08 and lower than 0.95. A linear plot of $\ln[(C_0/C_t)-1]$ against time (t) was employed to determine values of K_T and q_0 from the intercept and slope of the plot (Table 4). Values of R^2 were found to be > 0.946 .

It can be observed from Table 4 that the values of q_0 generally increased with an increase in the value of bed depth while the value of K_T decreased slightly. So higher bed depths would increase the rate adsorption of atenolol on the column.

A Yoon and Nelson empirical kinetic model (Yoon and Nelson, 1984) for a single component system is expressed as:

$$\ln\left(\frac{C_t}{C_0 - C_t}\right) = K_{Y-N} \cdot t - \tau \cdot K_{Y-N} \quad (9)$$

where K_{Y-N} (h^{-1}) is the rate velocity constant, τ (h) is the time required for C/C_0 is 0.50. A linear plot of $\ln[C_t/(C_0 - C_t)]$ against time (t) determined values of K_{Y-N} and τ from the intercept and slope of the plot (Table 4). The derivation of Eq. (9) was based on the definition that 50% breakthrough occurs at $t = \tau$. Thus, the

adsorption bed should be completely saturated at $t = 2\tau$. Owing to the symmetrical nature of breakthrough curves due to the Yoon-Nelson model, the amount of adsorbate being adsorbed in a fixed bed is half of the total adsorbate entering the adsorption bed within 2τ period. Hence, the following Equation can be obtained for a given bed:

$$q_0 = \frac{q_{(total)}}{w} = \frac{\frac{1}{2} C_0 [(Q/1000)(2\tau)]}{w} = \frac{C_0 \cdot Q \cdot \tau}{1000 \cdot w} \quad (10)$$

From Equation (10), adsorption capacity, q_0 , varies as a function of inlet atenolol concentration, C_0 , flow rate, Q , weight of adsorbent, w , and time required for C/C_0 is 0.50, τ . The values of K_{Y-N} and τ are listed in Table 4.

From Table 4, the rate constant K_{Y-N} does not show a clear trend, and the 50% breakthrough time τ increased clearly with increasing the bed depths. The data in Table 4 also indicated that τ values from the calculation were significantly higher compared to experimental results, 71, 147.7, and 151.7 h for bed depths of 8.0, 10.0 and 12.0 cm, respectively. Among the Thomas and Yoon-Nelson models, the value of correlation coefficients (R^2) listed in Table 4, both of them provide

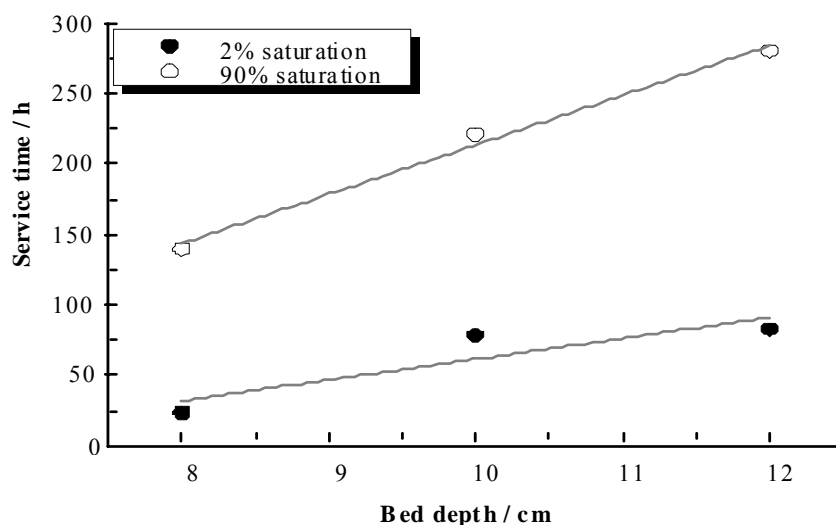


Fig. 4. Bed depth versus service time plot

Table 4. Thomas and Yoon-Nelson models parameters for fitting at different conditions using linear regression analysis

Initial concentration (mg/L)	Bed depth (cm)	Flow rate (mL/min)	Thomas Model				Yoon-Nelson Model				
			K_T (L/h/mg)	q_0 (mg/g)	R^2	S.E.	K_{Y-N} (h^{-1})	τ (h)	q_0 (mg/g)	R^2	S.E.
10	8.0	2.0	$3.5 \cdot 10^{-3}$	112.7	0.9547	2.96	2.5×10^{-2}	99.6	149.3	0.9733	10.60
10	10.0	2.0	$3.3 \cdot 10^{-3}$	187.4	0.9864	4.11	3.3×10^{-2}	156.2	181.4	0.9864	4.11
10	12.0	2.0	$2.8 \cdot 10^{-3}$	171.5	0.9458	2.34	2.8×10^{-2}	171.5	171.5	0.9458	2.34

a good fit ($R^2 > 0.93$) to the experimental parameters at different bed depths. In a comparison of values of R^2 and breakthrough curves, both the Thomas and Yoon-Nelson models can be used to describe the behaviour of the adsorption of atenolol in an activated carbon fixed bed column.

The standard error (SE) values were determined for the adsorption capacity obtained by Thomas and Yoon-Nelson model:

$$SE = \sqrt{\sum \frac{(q_{0(\text{exp})} - q_{0(\text{cal})})^2}{N}} \quad (11)$$

where, $q_{0(\text{exp})}$ is experimental adsorption capacity (Table 3), $q_{0(\text{cal})}$ is adsorption capacity calculated using theoretical kinetic models and N is the number of experimental points run. The values of SE are shown in Table 4. Comparison of the SE values calculated for the two models shows that although both fit reasonably well the adsorption data for the examined concentration range of atenolol. This contaminant presents a BET adsorption isotherm (Brunauer-Emmett-Teller model), which follows next Equation:

$$\frac{z}{n \cdot (1 - z)} = \frac{1}{n_m \cdot c} + \left(\frac{c - 1}{n_m \cdot c} \right) \cdot z \quad (12)$$

where $z = P/P_0$, P_0 is the vapour pressure of the pure condensate atenolol; n are the moles of atenolol adsorbed, and n_m are the moles of atenolol adsorbed on a complete monolayer. An operating line was drawn which was passing through the origin and the point given by C_0 and corresponding q_c . Fig. 5 shows the experimental and theoretical breakthrough curves according to Ramesh *et al.*, 2011. Comparison of the experimental breakthrough curves to the breakthrough profiles did not show a satisfactory fit. These curves follow a similar trend, but there is difference between these. A possible explanation is that it is assumed that the BET model isotherm is not a suitable model to determine the theoretical breakthrough curve by this way. The design was performed from breakthrough curve shown in Fig. 6 and next Equation, which relates the lengths of the experimental and industrial beds:

$$\frac{L_{\text{lab}}}{(t_4)_{\text{lab}}} = \frac{L_{\text{ind}}}{(t_r)_{\text{ind}} + \frac{\Delta t}{2}} \quad (13)$$

where L_{lab} is the length of the experimental bed, $(t_4)_{\text{lab}}$ is the time at which $C/C_0 = 0.50$, L_{ind} the length of the industrial bed, $(t_r)_{\text{ind}}$ is breakthrough time of the industrial bed, Δt is a parameter that relates the length of the mass transfer zone with the velocity of the front of concentration in the bed, $\Delta t = L_{\text{MTZ}}/v$, as it can be seen in Fig. 7. Therefore, data collected during laboratory tests serve as the basis for the design of

the industrial-scale adsorber. Equation (13) can be used only in cases where the length of the mass transfer zone, L_{MTZ} , and velocity of experimental tests, u , are the same as those used on an industrial scale. The experimental value of L_{MTZ} , and the velocity through the bed are 8.76 cm and 721.6 cm.h⁻¹, respectively. Therefore, this will be the design condition that will allow us to use the experimental data from breakthrough curve shown in Fig. 6 in the design of the industrial bed. The industrial bed will treat a flow rate of 10.0 m³.h⁻¹, using the continuity equation, the section of the industrial adsorber can be determined, taking into account that the velocity through the bed has to be constant:

$$S = \frac{Q}{u} \quad (14)$$

where S is the section of the industrial adsorber, Q is the volumetric flow rate, 10.0 m³.h⁻¹ and u is the velocity through the bed, 721.6 cm.h⁻¹. It can be obtained a section of 1.39 m², and therefore, a diameter of the adsorber of 1.32 m. Once the diameter of the adsorber had been calculated, an appropriate length for the mechanical design and operation of the bed has to be selected. This parameter is chosen based on two criteria: the contact time of the adsorbate in the bed and the pressure drop across the bed, which is usually less than 20% of operating pressure, which is 2 atm. Based on these design criteria an adsorber length of 3.0 m has been selected. The breakthrough time of the industrial adsorber, $(t_r)_{\text{ind}}$, which is the operating time of the adsorber, was determined, as mentioned, using Equation (13), where L_{lab} is the length of the experimental bed, 10 cm; $(t_4)_{\text{lab}}$ is the time at which $C/C_0 = 0.5$ and is determined from the breakthrough curve in Fig. 7, 48.5 h; L_{ind} the length of the industrial bed, 300 cm; Δt is a parameter that relates the length of the mass transfer zone, L_{MTZ} , with the velocity of the front of concentration in the bed, v ; $\Delta t = L_{\text{MTZ}}/v$. Therefore, the velocity of the front of concentration can be obtained from the expression: $v = L/t_4$. The values of v and Δt are 0.21 cm.h⁻¹ and 42.5 h, respectively. $(t_r)_{\text{ind}}$ is the breakthrough time of the industrial bed, that for described operating conditions was of 1352 h, 56 days.

CONCLUSION

The present investigation illustrates that the adsorption of atenolol from aqueous solutions on a fixed bed of granular activated carbon is an interesting and effective treatment for the removal of this micropollutant from waters. The adsorption process of atenolol was dependent on the bed height. It is found that the breakthrough time increases as the bed depth does. Parameters as adsorption capacity at breakthrough time (q_r) and saturation time (q_s), MTZ, FBU and removal percentage were obtained for three different column lengths. The removal of atenolol can

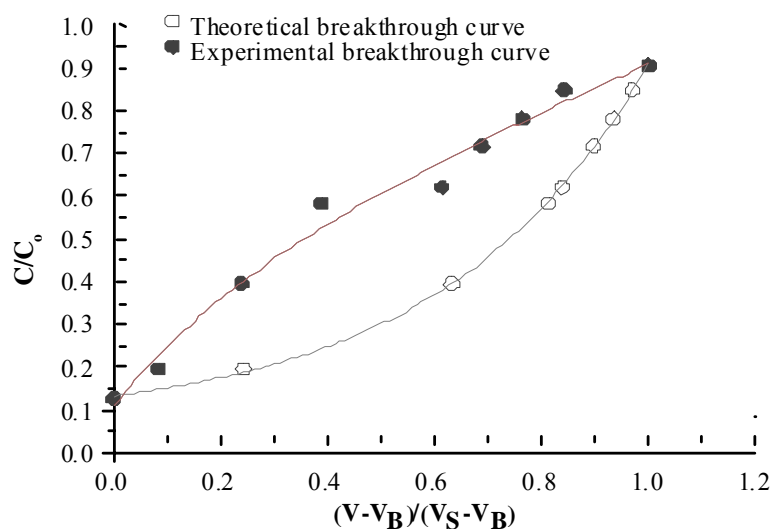


Fig. 5. Experimental and theoretical breakthrough curve of atenolol removal by GAC packed column

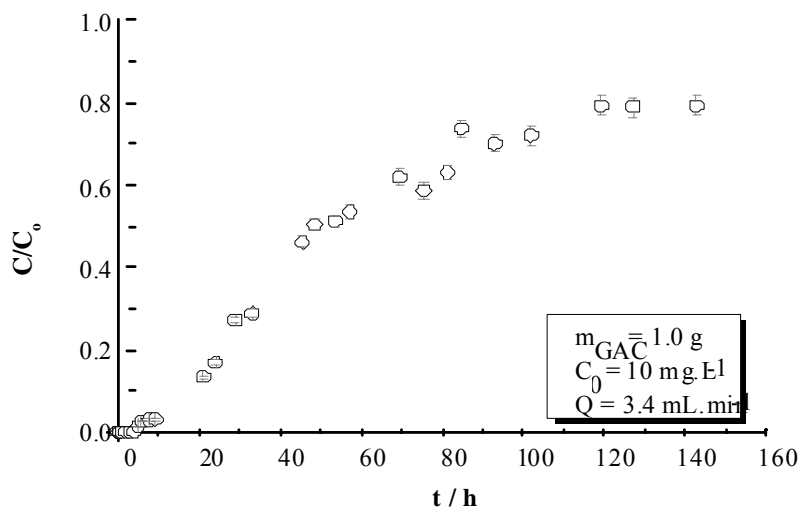


Fig. 6. Breakthrough curve of atenolol removal by granular activated carbon packed column of bed weight = 1.0 g, initial atenolol conc. = 10 mg.L⁻¹, flow rate = 3.4 mL.min⁻¹

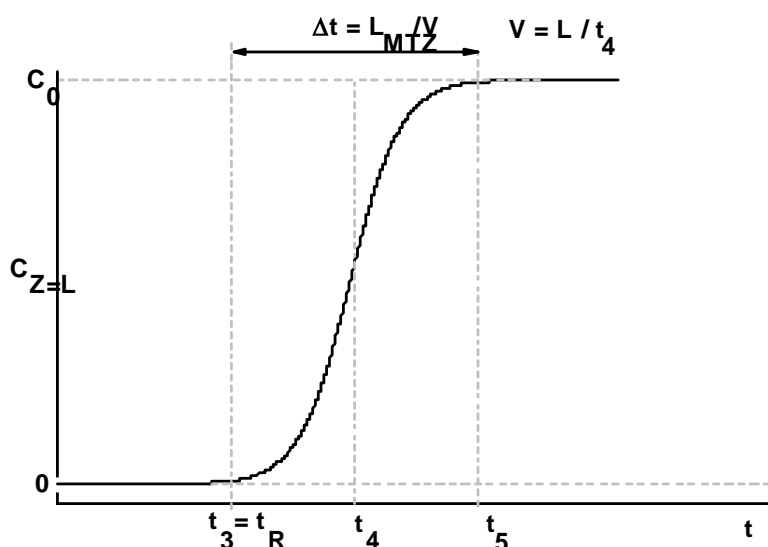


Fig. 7. Design parameters of an experimental breakthrough curve

be described by empirical models as Bohart-Adams, Thomas and Yoon-Nelson. These models show a good fitting for all examined range of breakthrough curves. Finally, an industrial-scale adsorber was scale up from experimental data of the breakthrough curves, as length of mass transfer zone and the velocity of the front of concentration in the experimental bed remain constant.

ACKNOWLEDGEMENT

The authors gratefully acknowledge the financial support from Ministerio de Educación y Ciencia by CONSOLIDER Program through TRAGUA Network CSD2006-44, CTQ2008-02728 and by Comunidad de Madrid through REMTAVARES Network S2009/AMB-1588.

REFERENCES

Akbarpour Toloti, A. and Mehrdadi, N. (2011). Wastewater Treatment from Antibiotics Plant. *Int. J. Environ. Res.*, **5** (1), 241-246.

Arvand, M., Vejdani, M. and Moghimi, M. (2008). Construction and performance characterization of ion selective electrode for potentiometric determination of atenolol in pharmaceutical preparations. *Desalination*, **225** (1-3), 176-184.

Beltrán, F. J., Pocostales, P., Álvarez, P. and Oropesa, A. (2009). Diclofenac removal from water with ozone and activated carbon. *J. Hazard. Mater.*, **163** (2-3), 768-776.

Benitez, F. J., Acero, J. L., Real, F. J., Roldan, G. and Casas, F. (2011). Comparison of different chemical oxidation treatments for the removal of selected pharmaceuticals in water matrices. *Chem. Eng. J.*, **168** (3), 1149-1156.

Bohart, G. S., Adams, E. Q. (1920). Some aspects of the behaviour of charcoal with respect to chlorine. *J. Am. Chem. Soc.*, **42**, 523-529.

Bolong, N., Ismail, A.F., Salim, M. R. and Matsuura, T. (2009). A review of the effects of emerging contaminants in wastewater and options for their removal. *Desalination*, **239**, 229-246.

Carballa, M., Omil, F. and Lema, J. M. (2008). Comparison of predicted and measured concentrations of selected pharmaceuticals, fragrances and hormones in Spanish sewage. *Chemosphere*, **72** (8), 1118-1123.

Giles, C. H. and Nakhwa, S. N. (1962). Studies in adsorption. XVI. The measurement of specific surface areas of finely divided solids by solution adsorption. *J. Appl. Chem.*, **12**, 266-273.

Gros, M., Petrović, M. and Barceló, D. (2006). Development of a multi-residue analytical methodology based on liquid chromatography-tandem mass spectrometry (LC-MS/MS) for screening and trace level determination of pharmaceuticals in surface and wastewaters. *Talanta*, **70** (5), 678-690.

Goel, J., Kadirlevu, K., Rajagopal, C. and Garg, V. K. (2005). Removal of lead(II) by adsorption using treated granular activated carbon: Batch and column studies. *J. Hazard. Mater.*, **125** (1-3), 211-220.

Hua, W., Bennett, E. R. and Letcher, R. J. (2006). Ozone treatment and the depletion of detectable pharmaceuticals and atrazine herbicide in drinking water sourced from the upper Detroit River, Ontario, Canada. *Water Res.*, **40** (12), 2259-2266.

Hutchins, R. A. (1973). New Method Simplifies Design of Activated Carbon Systems. *Chem. Eng.*, **80**, 133-138.

Klavarioti, M., Mantzavinos, D. and Kassinos, D. (2009). Removal of residual pharmaceuticals from aqueous systems by advanced oxidation processes. *Environ. Int.*, **35**, 402-417.

Kundu, S. and Gupta, A.K. (2007). Investigation on the kinetics and mechanism of sorptive removal of fluoride from water using alumina cement granules. *Chem. Eng. J.*, **129** (1-3), 123-131.

Lishman, L., Smyth, A.A., Sarafin, K., Kleywegt, S., Toito, J., Peart, T., Lee, B., Servos, M., Beland, M. and Seto, P. (2006). Occurrence and reductions of pharmaceuticals and personal care products and estrogens by municipal wastewater treatment plants in Ontario, Canada. *Sci. Total Environ.*, **367** (2-3), 544-558.

McKay, G. (1996). Use of adsorbents for the removal of pollutants from wastewaters, CRC Press, Boca Raton.

Postigo, C., López de Alda, M. J. and Barceló, D. (2010). Drugs of abuse and their metabolites in the Ebro River basin: occurrence in sewage and surface water, sewage treatment plants removal efficiency, and collective drug usage estimation. *Environ. Int.*, **36** (1), 75-84.

Radjenović, J., Petrović, M. and Barceló, D. (2009). Fate and distribution of pharmaceuticals in wastewater and sewage sludge of the conventional activated sludge (CAS) and advanced membrane bioreactor (MBR) treatment. *Water Res.*, **43** (3), 831-841.

Ramesh, S. T., Gandhimathi, R., Nidheesh, P. V., Badabhagani, N. and Bharathi, K.S. (2011). Breakthrough data analysis of adsorption of Cd (II) on coir pith column. *EJEAFChe.*, **10** (8), 2638-2658.

Sotelo, J. L., Uguina, M. A., Delgado, J. A. and Celemin, L. I. (2004). Adsorption of methyl ethyl ketone and trichloroethene from aqueous solutions onto activated carbon fixed-bed adsorbents. *Sep. Purif. Technol.*, **37** (2), 149-160.

Ternes, T.A., Meisenheimer, M., McDowell, D., Sacher, F., Brauch, H.-J., Haist-Gulde, B., Preuss, G., Wilme, U. and Zulei-Seibert, N. (2002). Removal of pharmaceuticals during drinking water treatment. *Environ. Sci. Technol.*, **36** (17), 3855-3863.

Thomas, H. C. (1944). Heterogeneous ion exchange in a flowing system. *J. Am. Chem. Soc.*, **66**, 1664-1666.

Vergili, I. and Barlas, H. (2009). Removal of selected pharmaceutical compounds from water by an organic polymer resin. *J. Sci. Ind. Res.*, **68**, 417-425.

Westerhoff, P., Yoon, Y., Snyder, S. and Wert, E. (2005). Fate of endocrine-disruptor, pharmaceutical, and personal care product chemicals during simulated drinking water treatment processes. *Environ. Sci. Technol.*, **39** (17), 6649-6663.

Yoon, Y. H. and Nelson, J. H. (1984). Application of gas adsorption kinetics II. A theoretical model for respirator cartridge service life. *Am. Ind. Hyg. Assoc. J.*, **45**, 509-516.